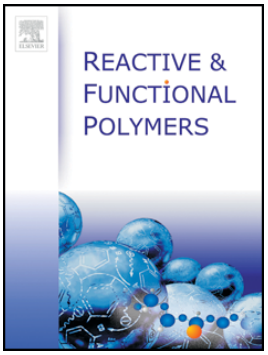

Antibacterial and antioxidant bio-based networks derived from eugenol using photo-activated thiol-ene reaction

Tina Modjinou, Davy-Louis Versace, Samir Abbad-Andallousi, Noureddine Bousserrhine, Pierre Dubot, Valérie Langlois, Estelle Renard

PII: S1381-5148(16)30021-9
DOI: doi: 10.1016/j.reactfunctpolym.2016.02.002
Reference: REACT 3630

To appear in:

Received date: 15 July 2015
Revised date: 2 February 2016
Accepted date: 2 February 2016

Please cite this article as: Tina Modjinou, Davy-Louis Versace, Samir Abbad-Andallousi, Noureddine Bousserrhine, Pierre Dubot, Valérie Langlois, Estelle Renard, Antibacterial and antioxidant bio-based networks derived from eugenol using photo-activated thiol-ene reaction, (2016), doi: 10.1016/j.reactfunctpolym.2016.02.002

Antibacterial and Antioxidant bio-based Networks derived from Eugenol using photo-activated thiol-ene reaction

Tina Modjinou [a], *Davy-Louis Versace* [a], *Samir Abbad-Andallousi* [b], *Noureddine Bousserrhine*[b], *Pierre Dubot* [a], *Valérie Langlois* [a], *Estelle Renard* [a*]

[a] Université Paris Est, ICMPE (UMR7182), CNRS, UPEC, F-94320 Thiais, France

[b] Université Paris-Est, Institut d'écologie et des sciences de l'environnement de Paris, Département SoléO, 61 avenue du Général de Gaulle, 94010 Créteil cedex, France

Keywords : eugenol, linalool, thiol-ene, antibacterial network, antioxidant properties

Abstract

Bio-based networks derived from eugenol and linalool were prepared with an eco-friendly process by photoactivated thiol-ene reactions. Allyl derivative Eugenol, ***AE,*** prepared by a nucleophilic substitution was combined with linalool, ***L***, a monoterpene presents in the lavender essential oil, well known to its antibacterial activity or with Eugenol, ***E***, a sustainable antioxidant molecule major component of the essential oil of clove. The photoactivated thiol-ene reaction is a quick room temperature straightforward way to obtain renewable crosslinked networks. Two bacteria strains were used *in vitro* to evaluate the resistance to bacterial adhesion and the DPPH method was used to determine the antioxidant properties of the networks. As expected, the results showed a promising anti-adhesion activity against *S. aureus* and *E. coli* due to the presence of eugenol moieties. Moreover, the phenol groups of eugenol provide an antioxidant activity characterized by a radical scavenging activity of 90%.

Introduction

Nowadays, industrial chemicals and materials are mainly derived from fossil resources that are both less available and a a major source of greenhouse gas emissions. The challenges of reducing the emissions of CO_2, and more generally, the impacts on the environment, weigh more and more in balance of the governments, industries and consumers. The share of renewable carbon in the products of the chemical industry should raise 15% in 2017 against 7% today [1]. In the same way, American studies estimate that 90% of organic chemical products will be based on renewable resources by 2090 [2]. Therefore, it is crucial to propose new renewable resources as an alternative of petrochemical products especially for the polymer industry. Various monomers derived from bio-sourced materials (starch, cellulose, vegetal oils…) are already used for the production of polymers [3] but the monomers obtained by bio-refinery process are only aliphatic or cycloaliphatic componds. The bio-based aromatic compounds can be extracted from the lignin or tannins but their industrial valorisation is limited by their structural complexity. Currently, only vanillin is industrially extracted from the lignin and consequently a variety of high performance resins [4, 5] and polymers [6, 7] have been recently developed with the derivatives of vanillin. The essential oils constitute another source of free mono-aromatic compounds having a large spectrum of chemical structures. Among them, Eugenol extracted from the clove oil is a very interesting phenolic compound, readily available which can be considered as an inexpensive functional monomer. The presence of two functional groups, a vinyl and a phenol group,

allowed the preparation of polyacetylenes [8, 9], aromatic copolyesters [10] and multiblock copolymers [11]. A variety of eugenol derivatives including the bisphenol [12], bisepoxy [13], allyl-etherified eugenol [14, 15] or methacrylic derivatives have also been used to prepare renewable resins [16]. The biological properties of eugenol are used for a long time in dentistry [17-20] to prepare dental resins. The terpenes are also abundant and inexpensive bio-based molecules. Several recent publications report the incorporation of essential oils as additives to prepare active packaging [21-24]. Linalool, ***L***, is an oxygenated terpenoid, that has very attractive antibacterial properties [25-29]**.**

In this context, we prepared UV-cured networks by using thiol-ene formulation with allyl eugenol, ***(AE),*** Eugenol ***(E)*** or Linalool ***(L)*** as shown in **Scheme 1**. To overcome the problem of the diffusion of antibacterial molecules over time, it is worth considering to covalently link these molecules to ensure a more sustainable antimicrobial property. The main challenge of our study is, on the one hand, assuming the preservation of the antibacterial property of the cross-linked eugenol and, on the other hand, to enhance the activity by using eugenol **(*E*)** and linalool **(*L*)**. The covalent insertion of eugenol in the network should enhance the antibacterial and antioxidant properties thanks to the presence of phenol groups. Moreover, the introduction of an anti-bacterial acyclic monoterpene, linalool, should modulate the mechanical properties of the material. The thermomechanical properties of these materials were investigated and the effects of the composition are discussed. Their antioxidant activity and their action against bacterial adhesion are tested by using against the both pathogenic mono-species, *Staphylococcus aureus* and *Escherichia coli.*

Experimental

Materials

Trimethylolpropane tris(3-mercaptopropionate) ≥ 95% (Trithiol), linalool (***L***) 97% and potassium carbonate (K_2CO_3) 99% were purchased from Aldrich. Eugenol (***E***) 99% and allyl bromide 99% stab. with 300-1000 ppm propylene oxide were obtained from Alfa Aesar. 2,2-dimethoxy-1,2-diphenylethan-1-one (DMPA) was provided by BASF company. N,N-dimethylformamide anhydrous, methanol and ethyl acetate were purchased from Carlo Erba Reagents. 2,2-diphenyl-1-picrylhydrazyl (DPPH) and Lysogeny Broth, Miller (LB medium) were purchased from Aldrich. Other chemicals for this study were analytic reagents obtained from Aldrich and used without purification.

Instrumentation

^{1}H NMR (400 MHz) spectra were recorded on a Brucker AV 400M in $CDCl_3$ at 25°C. FT-IR spectra were recorded on a Brucker Tensor 27 spectrometer with 32 scans equipped with an ATR apparatus. Measurements were performed on a Horiba Xplora confocal Raman microscope (Horiba Jobin Yvon) equipped with an external excitation source (638 nm He-Ne laser). The objective lenses used in the study were 50x long-working distance (Long Working Distance M Plan Semi-Apochromat, LMPLFL50x, Olympus) and 10x (M Plan Achromat, MPLN10x, Olympus), operating in air. Spectral acquisition was obtained using LabSpec software (Horiba Scientific, Edison, New Jersey). Raman spectra were recorded at a resolution of 1 cm^{-1} in the range between 4000 and 200 cm^{-1}. Repeated acquisitions using the highest magnification were accumulated to improve the signal-to-noise ratio. Spectra were calibrated using the 520.5 cm^{-1} line of a silicon wafer. Spectral details were as following; objective: × 50, filter: 100 %, exposition: 10, slit: 50, hole: 500. Spectra were averaged from two to five accumulations, each with an acquisition time ranging from 15 s to 5 min. The conditions of measurement were adjusted depending on the type of the matrices to obtain a good signal-to-noise ratio.

X-ray photoelectron (XPS) measurements were made with a Thermo Scientific K-Alpha apparatus. Survey scans were done using a monochromatic Mg Kα X-ray source (12 KeV, 2 mA) with a spot diameter of 25 mm^2 operated in a low power mode (24 W). A pass energy of 10 eV was used for the detailed XPS scans. XPS spectra were obtained with an energy step of 0.05 eV with a dwell time of 200 ms. Data acquisitions have mainly been focused on the C1s, O1s core level lines. The spectra obtained were treated by means of the “Avantage” software provided by ThermoFisher. The C1s and O1s envelopes were analyzed and peak-fitted using Gaussian line shapes. The binding energy scale was fixed by assigning a binding energy of 284.8 eV to the−CH− carbon (1s) peak.

Water contact measurements were performed with the Drop Shape Analysis system Krûss Easy DROP Contact Angle measuring system apparatus controlled by the DSA software.

The thermal properties of the networks were measured by Differential Scanning Calorimetry (DSC). The measurements were conducted on Perkin Elmer Diamond DSC apparatus according to the following heating programs: heating from −60 to 170°C at 20°C.min^{-1}, cooling to −60°C at 200°C.min^{-1} holding at 60°C for 5 min and heating to 170°C at 20°C.min^{-1} to determine the glass transition temperatures. Thermogravimetric analyses (TGA) were performed on a Setaram Setsys Evolution 16 apparatus by heating from 20°C to 800°C at 10°C.min^{-1} under argon atmosphere. Mechanical properties were conducted at room

temperature on an Instron 5965 apparatus equipped with a 20mN sensor at a crosshead displacement rate of 1mm.min^{-1}.

Preparation and characterization of the samples

*Synthesis of allyl-eugenol (**AE**)*

Allyl-eugenol was synthesized by the Williamson reaction. Eugenol (2 g, 1.2.10^{-2} mol) was dissolved in 20 mL of N,N-dimethylformamide and 2eq of K_2CO_3 were added. The mixture was cooled in an ice bath. The solution became yellow and turned green. Allylbromide (2 eq) were added dropwise by a funnel and the solution was stirred for 72h. Then, a large volume of water was added and the solution was stirred 30min. Finally, the solution was several extracted with ethyl acetate and the organic layer was washed with water, then dried under $MgSO_4$ and concentrated to give the final yellow liquid product with a yield of 90%. The ^{1}H NMR spectrum (**Fig. 1**) shows the appearance of new signals at 5.96, 5.39 and 5.26 ppm characteristic of unsaturated allyl groups derived from etherification reaction of eugenol which confirms the success of the reaction. The etherification reaction was quantitative as indicated by the ratios of both alkene groups.

*Allyl-eugenol/eugenol networks preparation, **AE/E** networks*

As an example, the synthesis of 70-30 (w/w%) ***AE/E*** network (1eq SH/C=C) is described here. ***E*** (84µL, 90 mg, 4.4.10^{-4} mol) and DMPA (3% w/w) were dissolved in ***AE*** (210 mg, 1.3.10^{-3} mol). Trithiol (429 mg, 1.1.10^{-3} mol, 1eq. SH/C=C) were added to the solution. The formulation was poured into a silicone mould (1.8 x 4 cm) and heated at 60°C during at least 1h then irradiated 5 min at room temperature by Lightning LC8 (L8251) from Hamamatsu equipped with a mercury-xenon lamp (200W) coupled with a flexible light guide. The end of the guide was placed at 11cm of the sample to give the transparent and flexible resulted material. The maximum UV light intensity at the sample position was measured by radiometry (International Light Technologies ILT 393) to be 180 mW.cm^{-2} in the 250-450 nm. The extent of conversion was measured via FT-Raman spectroscopy from the band 2600 cm^{-1} corresponding to the SH bonds after the normalization of the spectrum to the ester carbonyl peak at 1735 cm^{-1}. The relative conversion α was calculated according to the following equation:

$$\text{(eq. 1)} \qquad \alpha = \left(\frac{R_0 - R_t}{R_0}\right) \times 100$$

With $R_0 = \frac{I_{SH}}{I_{C=O}}$, before irradiation and $R_t = \frac{I_{SH}}{I_{C=O}}$, after irradiation

Water uptake determination

Prior to the water uptake measurements, the samples were dried under vacuum. They were placed in a conditioning closed chamber over a saturated solution of NaCl to obtain a water saturated atmosphere of 75% at room temperature. The percentage uptake of moisture into the material was measured by a coulometric method at t = 0 s and after 18 h. The 831 K F Coulometer Metrohm was equipped with a 728 Stirrer and an 860 KF Thermoprep Metrohom.

Soluble extract determination

The samples were treated with 10 mL of diethyl ether stirred in a flask during 3h at room temperature. The remaining residue and the film were weighted after the solvent evaporation under vacuum.

*Real Time Fourier Spectroscopy kinetics of allyl eugenol **AE** conversion in network formed by photochemistry*

Kinetics of the photo-addition reactions were followed by Real-Time Fourier Transform Infra Red Spectroscopy (RT-FTIR) using a Thermo-Nicolet 6700 instrument and a 80µL of a liquid mixture composed of ***AE***, ***L*** or ***E*** and trithiol. The photoinitiator (DMPA) was dissolved to a 3% w/w dilution. This sample was applied to a BaF_2 chip by a calibrated wire-wound applicator. The thickness of the UV curable film was evaluated at 4 µm. The RT-FTIR analyses were carried out under laminated conditions: a polypropylene film was deposed on the top of the photosensitive layer to prevent oxygen diffusion. Samples were simultaneously exposed for a few seconds to both the UV beam, which starts the photoreaction, and the IR beam which analyzes the extent of the photoreaction in situ. The mixture was irradiated at room temperature with the Hamamatsu lightening cure LC8 (L8251), equipped with a Mercury-Xenon lamp (200 W) coupled with a flexible light guide. The end of the guide was placed at a distance of 11 cm of the sample's surface. The light intensity on the surface of the sample was about 180 mW. cm^{-2}. The thiol-ene photo-addition was monitored by the disappearance of the C=C bonds of (***AE***) at 1647 cm^{-1} and of the SH bonds of the trithiol at 2560 cm^{-1}.

Bacterial adhesion

The anti-adherence activity of the networks was evaluated using two pathogenic bacterial strains: *Staphylococcus aureus* ATCC6538 (Gram- positive) and *Escherichia coli* ATCC25922 (Gram- negative) which were grown aerobically at 37°C overnight on LB medium before the bacterial adhesion tests. The samples of ***AE***-based networks were immersed 1h at 37°C and stirred in the bacterial suspension of the two different strains (OD_{600nm} = 0.05). The non-adherent bacteria were then removed from the network surface by several washes with a physiological saline buffer. The networks were then submitted to vortex and ultrasounds in a minimum volume of saline buffer to unhook fasten bacteria. Finally, 100 µL of this resulting viable bacteria suspension were inoculated onto the surface of a PCA agar (Plate Count Agar) Petri dish. After 24h of incubation at 37°C in aerobic conditions, the antibacterial activity was measured by counting the overall number of bacteria (CFU-Colony Forming Units) for the different strains. Each experiment was performed in six replicates. The software R was used to analyse the data. At least, six replicates of the experiments were conducted in order to allow a significant statistical analysis. The ANalysis Of the VAriance (ANOVA) statistical test was used and significant differences ($p < 0.05$) among antibacterial properties of the networks were detected thanks to the multiple range test of Duncan.

Antioxidant Activity

The antioxidant activity of the networks was determined according to the DPPH (2,2-diphenyl-1-picrylhydrazyl) method [22, 30-32]. About 100mg of the network were immersed in 4mL of 0.1mM DPPH solution (in methanol). This solution was then left in the dark for 60min at room temperature. The radical scavenging activity was measured by using a Varian Cary 50 Bio UV-Visible spectrophotometer controlled by the CaryWinUV software. The DPPH solution is well known to have a maximum of absorption at 517nm. The antioxidant activity was therefore determined by monitoring the decrease of the absorbance at this wavelength. The radical scavenging activity was calculated according to the following equation:

(eq. 2) $$Radical\ scavenging\ activity\ (\%) = \left(\frac{A_{ref}\text{-}A_s}{A_{ref}}\right) \times 100$$

where A_{ref} corresponds to the absorbance of the 0.1mM DPPH solution without network and A_s corresponds to the absorbance of the 0.1mM solution of DPPH with the network at 517nm.

Results and discussion

Preparation of networks

This study entails the design of photoinduced thiol-ene networks based on allyl-eugenol (***AE***), eugenol (***E***) or linalool (***L***) in presence of DMPA (**Scheme 1).** The first step consisted in the synthesis of allyl eugenol (***AE***) by reaction of eugenol with allyl bromide. The eugenol networks were prepared by thiol-ene reaction of unsaturated ***AE*** with the trithiol in presence of DMPA as photoinitiator under UV irradiation. This procedure is an easy synthetic methodology for the preparation of networks with variable properties as it was previously described [33]. For this study, materials containing different percentage of ***AE,*** from 50 to 100%, were prepared. For all compositions studied, the initial stoichiometry C=C/SH was maintained to 1/1. **Figure 2** shows the FT-IR spectra of the mixture ***E***, ***AE*** and **AE/E** (***70/30)*** before irradiation. The stretching band of C=C groups for both ***AE*** and ***E*** appears at 1647 cm^{-1} and the absorption of the SH groups is identified at 2560 cm^{-1}. The success of the reaction was confirmed by the decrease of the SH bond after irradiation. The kinetics profiles of the disappearance of the SH functions was determined (**Fig. 3**). After 50s of irradiation, high conversion(80-85%) of SH were obtained, confirming the efficacy and the high speed of the reaction. Raman spectroscopy has been also used to follow the cross-linking process of the different compositions. **Figure 4** shows a characteristic peak at 1700 cm^{-1} for the carbonyl group and a strong characteristic peak at 2570 cm^{-1} . The conversion is determined by comparison of the intensities of these bonds. Different samples were prepared by varying the percentage of linalool from 0 to 100%.

In the case of the monofunctional eugenol, only 30% can be added since higher amounts led to a insufficient crosslinking . Nevertheless, the content of linalool can reach 50% thanks to the presence of the two double bonds able to react by thiol-ene reaction. As reported in **Table 1**, the conversion of SH group, determined by Raman spectroscopy was higher than 90 % in comparison with the one measured in laminated conditions by FTIR (80-85%). This difference can be explained by the difficulty to monitoring the SH band by Real-Time FTIR due to the weakness of the SH band. However, despite the stoichiometry, a total conversion was not achieved. By contrast, the study of the soluble extract (< 5%) highlighted a high cross-linking density. The non-quantitative conversion may due to the decrease of the molecules mobility at high conversion that diminishes the access to reactive groups.

Characterization of the networks

As expected, the water contact angle diminishes from 73° to 62° with the decrease of the aromatic moieties amount from 100% to 50% (**Table 2**). To investigate the presence of functional groups to the surface of the networks, XPS analyses were performed. The deconvolution of the C1s band (**Fig.5**) reveals that ***AE/L*** (***70/30*** and ***50/50***) and ***AE/E*** (***70/30***) are composed of five peaks. **Table 3** presents the values of binding energy and the relevant content of the functional groups. Based on the value of binding energy, the peaks at 284.3, 284.8, 285.7, 286.4 and 289.2 eV are attributed to C-C aromatic (A), C-C/C-H aliphatic (B), C-OH phenolic and aromatic ether (C), C-OH and aliphatic ether (D), and C=O (E) respectively. The assignments are in agreement with the literature [34-37] and the C-S peak cannot be distinct in the spectra due to the overlap by the C-C peak [38]. For 100% ***AE***, an additional peak appears corresponding to the π-π* transitions of the aromatic carbon at 289.5 eV (F). As reported in the **Table 3**, the intensities of the peaks C and D corresponding to both C-O (aromatic and aliphatic) are higher for ***AE*** network than those obtained in the case of the ***AE/E*** (***70/30***) network. This is in line with the chemical structure of ***AE*** that contains two types of $C_{aromatic}$-O-$C_{aliphatic}$ bonds. The C1s peaks of ***AE/L*** are quite similar to those of the ***AE/E***, but the ratio D/C in ***AE/L*** networks is higher than those obtained in the ***AE/E*** material. This ratio increases slightly with the linalool content suggesting that the hydroxyl groups from linalool are located at the surface. In the same way, for an equal proportion of eugenol (**Fig.5b-5c**) the peak C is higher for the ***AE/E*** network in comparison with the ***AE/L*** meaning that phenol groups are present at the surface. They should play a valuable role in the biological properties.

Furthermore, the water sensitivity of the networks was investigated by measuring the amount of water taken up by conventional Karl Fisher titration. The water uptakes remained lower than 5% after 18h of exposition to an atmosphere containing 75% of relative humidity indicating that the samples were not sensitive to water. These results can be explained by the presence of aromatic moieties coming from the eugenol. Thus, the mechanical integrity will be preserved after being exposed to an aqueous medium and no degradation reactions will be occurred.

Mechanical and thermal properties were investigated and reported in **Table 2**. The formation of flexible thioether linkages induces low glass transition temperatures (< 0°C) as reported previously [39-41]. The Tg values do not vary significantly with the composition of the networks suggesting that the cross-linking density is similar. Thermal degradation was determined by TGA by considering the temperature corresponding to 5% of mass loss. The thermal degradation temperatures of ***AE/L*** and ***AE/E*** networks were between those of linalool

and ***AE*** networks. The presence of ***AE*** aromatic units increases the thermal stability. The determination of the Young's modulus (E), the strain (ε) and the tensile stress (σ_r) were performed. The mechanical results obtained from stress-strain curves are listed in **Table 2** and presented in **Figure 6**. Similar trends were observed in the strain and the tensile stress values of the materials, reflecting the relation between the presence of the linear soft linalool units and the crosslink density. The introduction of the monofunctional eugenol in the formulation leads to a reduction in the mechanical properties due to a decrease of crosslinking density.

Anti-adhesion activity

The anti-adhesion properties of the networks were studied with the two strains of bacteria after 1h of incubation in the bacterial suspension. **Figure 7** shows the number of adhered bacteria (CFU/cm^2) calculated by the ANOVA and StatAdvisor post-tests. The bacterial adhesion depends on the strains of the bacteria. The CFU/cm^2 values of *S. aureus* were systematically lower than those obtained with *E.coli*. These results indicate that the systems based on ***AE*** alone or associated with eugenol or linalool present intrinsic antibacterial properties. Indeed, the adhesion is lower in presence of eugenol derivatives, indicating that the presence of the aromatic moieties induces an increase of the antibacterial efficiency. It can be assumed that the decreasing of the bacterial adhesion can be related to the higher hydrophobicity of the ***AE*** networks. The presence of linalool led to a lower efficiency towards the bacteria adherence. Presumably, these results are partly linked to the presence of the aromatic derivatives and are independent of the hydroxyl amounts. *S. aureus* exhibits a preference for the attachment on hydrophobic surfaces [42, 43] and, the anti-adherence activity showed here can be explained by the presence of the aromatic moieties of the eugenol. Furthermore, the phenol group in the ***AE/E 70/30*** networks showed an improved anti-adhesive property as it was reported in the case of free eugenol [44, 45]. The presence of 30 wt % of eugenol in the ***AE*** networks decreased the CFU cm^{-2} values of 57% for *S. aureus* strains. There was no statistically significant difference for *E.coli* according to the ANOVA statistical test. The ***AE*** networks exhibit a promising anti-adhesive property which was not significantly improved by introducing 30 wt % of eugenol **(Fig.7)**.

Antioxidant activity

DPPH is a free radical widely used to determine the antioxidant activity of molecules [22, 30, 31, 46, 47]. Indeed, when this radical having a maximum of absorption at 517 nm, reacts with an hydrogen donor such as antioxidant, the absorbance decreases [48] and consequently there

is a discoloration of the solution from purple to pale yellow. The results of the antioxidant activity of the networks are shown in **Figure 8**. An increase in the presence of phenol groups in the networks led to an increase of the activity from 23% to 90% for the ***AE*** and ***AE/E*** (***70/30***) networks respectively. These results confirmed by the discoloration of the DPPH solution show the importance of the presence of phenol group for keeping an antioxidant activity.

Conclusions

The powerful and green process of thiol-ene addition was used to design solvent-free bio-based networks from eugenol and linalool. The transparent networks from sustainable compounds were successfully synthesized. The photoinitiated thiol-ene addition of allyl-eugenol ***AE*** and linalool ***L*** or eugenol ***E*** is a straightforward and efficient route to design renewable networks with a high crosslinking density. Moreover, the anti-bacterial properties against *S.aureus* and *E. coli* were particularly significant for the ***AE/E*** (***70/30***) network. The presence of 30 % of native eugenol with free phenol moieties promotes the anti-adhesion activity and leads to anti-oxidant properties. Finally, the new bio-based materials are not affected by water penetration under high moisture conditions. Eugenol represents a very promising compound for the elaboration of new bio-based networks. The intrinsic antibacterial and antioxidant properties of this compound could be very interesting in many fields such as food packaging.

AUTHOR INFORMATION

Corresponding Author

* Phone: 33 (0)1 49 78 12 17. E-mail: renard@icmpe.cnrs.fr.

Acknowledgment

We would like to thanks CNRS and UPEC for financial support. The authors thank the French Ministry of Research for providing Tina Modjinou with a grant.

References

[1] http://www.europabio.org.
[2] M. Eissen, J.O. Metzger, E. Schmidt, U. Schneidewind, Angew. Chem. Int. Ed., 41 (2002) 414-436.
[3] N. Berezina, S.M. Martelli, Bio-based polymers and materials, in: Renewable Resources for Biorefineries, ROYAL SOCIETY OF CHEMISTRY, 2014, pp. 1-28.
[4] C. Aoufa, S. Benyahyab, A. Esnoufa, S. Caillolb, B. Boutevinb, H. Fulcranda, European Polymer Journal, 55 (2014) 186-198.
[5] C. Aouf, E. Durand, J. Lecomte, M.-C. Figueroa-Espinoza, E. Dubreucq, H. Fulcrand, P. Villeneuve, Green Chem., 16 (2014) 1740-1754.
[6] L. Mialon, R. Vanderhenst, A.G. Pemba, S.A. Miller, Macromol. Rapid Com., 32 (2011) 1386-1392.
[7] F. Pion, A.F. Reano, P.-H. Ducrot, F. Allais, RSC Adv., 3 (2013) 8988-8997.
[8] E.A. Rahim, F. Sanda, T. Masuda, Journal of Polymer Science Part A: Polymer Chemistry, 44 (2006) 810-819.
[9] E.A. Rahim, F. Sanda, T. Masuda, J. Macromol. Sci., Part A: Pure Appl. Chem., 41 (2004) 133-141.
[10] P.B. Waghmare, S.B. Idage, S.K. Menon, B.B. Idage, Journal of Applied Polymer Science, 100 (2006) 3222-3228.
[11] P. Majumdar, A. Chernykh, H. Bao, E. Crowley, S. Zhang, J. Bahr, M. Weisz, C. Ulven, T. Zhou, R.B. Moore, B.J. Chisholm, Polymer Engineering & Science, 54 (2014) 1648-1663.
[12] B.G. Harvey, A.J. Guenthner, G.R. Yandek, L.R. Cambrea, H.A. Meylemans, L.C. Baldwin, J.T. Reams, Polymer, 55 (2014) 5073-5079.
[13] H. Qin, H. Liu, S. Zhang, M. Wolcott, S. Zhang, Polym. Int., 63 (2014) 760-765.
[14] T. Yoshimura, T. Shimasaki, N. Teramoto, M. Shibata, European Polymer Journal, 67 (2015) 397-408.
[15] M. Neda, K. Okinaga, M. Shibata, Materials Chemistry ans Physics, 148 (2014) 319-327.
[16] L. Rojo, B. Vazquez, J. Parra, A.L. Bravo, S. Deb, J. San Roman, Biomacromolecules, 7 (2006) 2751-2761.
[17] F.D. Sticht, R.M. Smith, J. DENT. RES, 6 (1971) 1531-1535.
[18] G.M. Laekeman, L. van Hoof, A. Haemers, D.A. Vanden Berghe, A.G. Herman, A.J. Vlietinck, Phytother. Res., 4 (1990) 90-96.
[19] A.E. Kaplan, M. Picca, M.I. Gonzalez, R.L. Macchi, S.L. Molgatini, Dent. Traumatol., 15 (1999) 42-45.
[20] J. Feng, J.M. Lipton, Neuropharmacology, 26 (1987) 1775-1778.
[21] M.L. Robertson, J.M. Paxton, M.A. Hillmyer, ACS Appl. Mater. Interfaces, 3 (2011) 3402-3410.
[22] M. Jouki, F.T. Yazdi, S.A. Mortazavi, A. Koocheki, Food Hydrocolloids, 36 (2014) 9-19.
[23] M.P. Arrieta, J. Lopez, A. Hernandez, E. Rayon, European Polymer Journal, 50 (2014) 255-270.
[24] J.M. Bolton, M.A. Hillmyer, T.R. Hoye, ACS Macro Lett., 3 (2014) 717-720.
[25] Z. Habibi, M. Yousefi, M. Mohammadi, F. Eftekhar, T. Biniyaz, A. Rustaiyan, Chemistry of Natural Compounds, 46 (2010) 819-821.
[26] I. Kubo, K.-I. Fujita, A. Kubo, K.-I. Nihei, T. Ogura, J. Agric. Food Chem., 52 (2004) 3329-3332.
[27] P. Lo Cantore, N.S. Iacobellis, A. De Marco, F. Capasso, F. Senatore, J. Agric. Food Chem., 52 (2004) 7862-7866.
[28] S.-N. Park, Y. Kyong Lim, M. Oliviera Freire, E. Cho, D. Jin, J.-K. Kook, Anaerobe, 18 (2012) 369-372.
[29] N.S. Iacobellis, P. Lo Cantore, F. Capasso, F. Senatore, J. Agric. Food Chem., 53 (2005) 57-61.
[30] S. Zouari, M. Ketata, N. Boudhriouna, E. Ammar, Industrial Crops and Products, 41 (2013) 172-178.

[31] A.J. Kirby, R.J. Schmidt, Journal of Ethnopharmacology, 56 (1997) 103-108.
[32] A.E.H. Youbi, D. Bousta, B. Jamoussi, H. Greche, L. Mansouri, J. Benjilali, S.H. Soidrou, Phytothérapie, 10 (2012) 151-160.
[33] C. Lorenzini, D.L. Versace, C. Gaillet, C. Lorthioir, S. Boileau, E. Renard, V. Langlois, Polymer, 55 (2014) 4432-4440.
[34] D. Downarowicz, Adsorption, 21 (2015) 87-98.
[35] S. Reiche, R. Blume, X.C. Zhao, D. Su, E. Kunkes, M. Behrens, R. Schlogl, Carbon, 77 (2014) 175-183.
[36] B. Yu, X. Wang, W. Xing, H. Yang, X. Wang, L. Song, Y. Hu, S. Lo, Chemical Engineering Journal, 228 (2013) 318-326.
[37] C. Zhu, S. Guo, Y. Fang, S. Dong, ACS Nano, 4 (2010) 2429–2437.
[38] J. Huang, W. Xu, Applied Surface Science, 256 (2010) 3921-3927.
[39] I. Carlsson, A. Harden, S. Lundmark, A. Manea, N. Rehnberg, L. Svensson, in: P.S.C. AB (Ed.) Photoinitiated Polymerization, ACS Symposium Series, 2003, pp. 65-75.
[40] M. Claudino, J.-M. Mathevet, M. Jonsson, M. Johansson, Polym. Chem., 5 (2014) 3245-3260.
[41] M. Sangermano, G. Colucci, M. Fragale, G. Rizza, Reactive & Functional Polymers, 69 (2009) 719-723.
[42] K. Bazaka, M.V. Jacob, V.K. Truong, R.J. Crawford, E.P. Ivanova, Polymers, 3 (2011) 388-404.
[43] N.R. James, A. Jayakrishnan, Biomaterials, 24 (2003) 2205–2212.
[44] F. Chen, Z. Shi, K.G. Neoh, E.T. Kang, Biotechnology and Bioengineering, 104 (2009) 30-39.
[45] S.A. Burt, Int. J. Food Microbiol., 94 (2004) 223-253.
[46] C. Sanchez-Moreno, Food Science and Technology International, 8 (2002) 121-137.
[47] M. Hajji, O. Masmoudi, N. Souissi, Y. Triki, S. Kammoun, M. Nasri, Food Chemistry, 121 (2010) 724-731.
[48] K. Shimada , K. Fujikawa , K. Yahara , T. Nakamura, J. Agric. Food Chem., 40 (1992) 945–948.

Scheme 1. Synthesis of the allyl-eugenol ***AE*** and the formation of the allyl-eugenol */eugenol* ***AE/E*** or allyl-eugenol */linalool* ***AE/L*** networks by thiol-ene reaction.

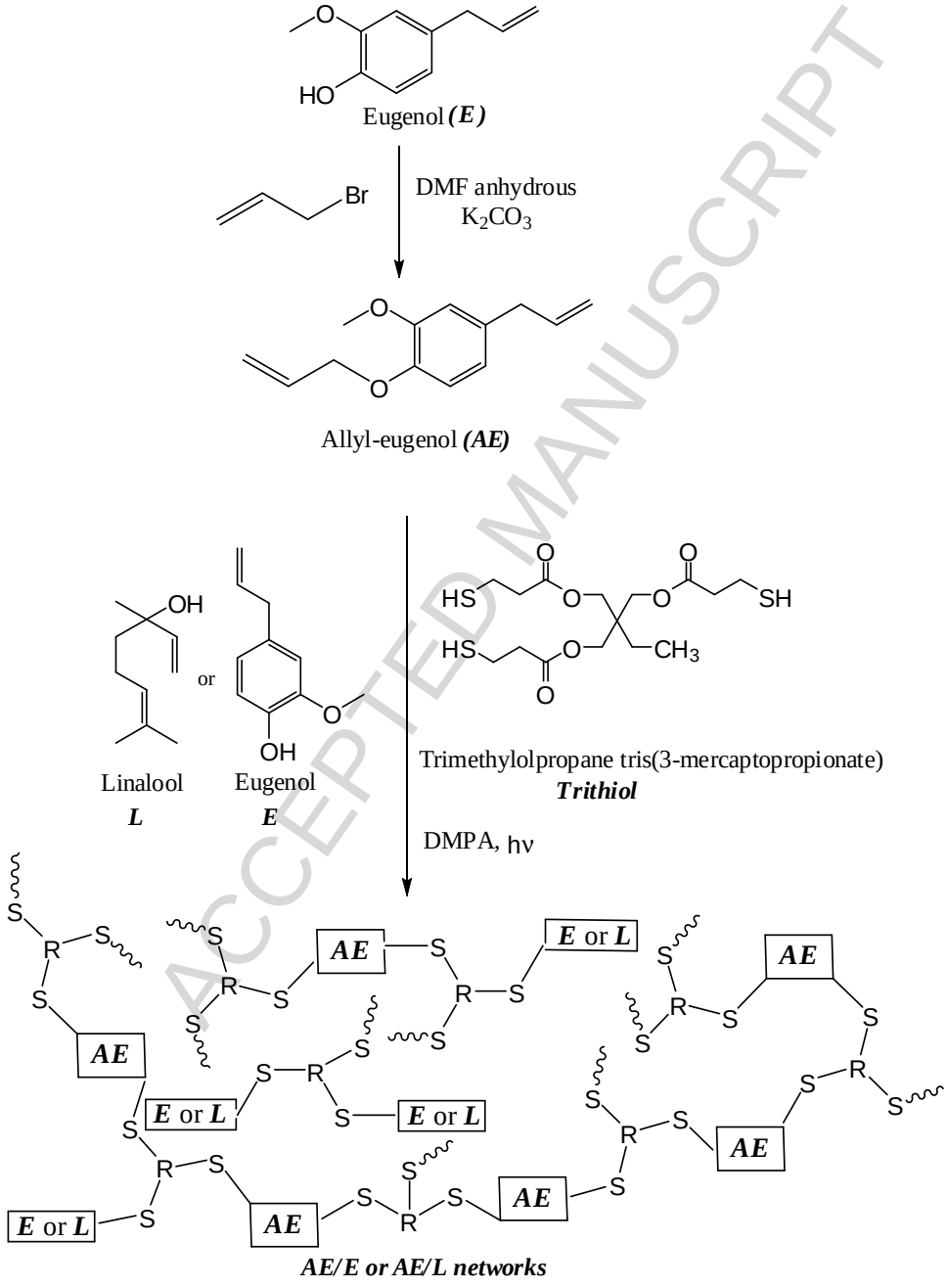

Figure 1. ^{1}H NMR spectrum of allyl-eugenol ***AE*** in $CDCl_3$.

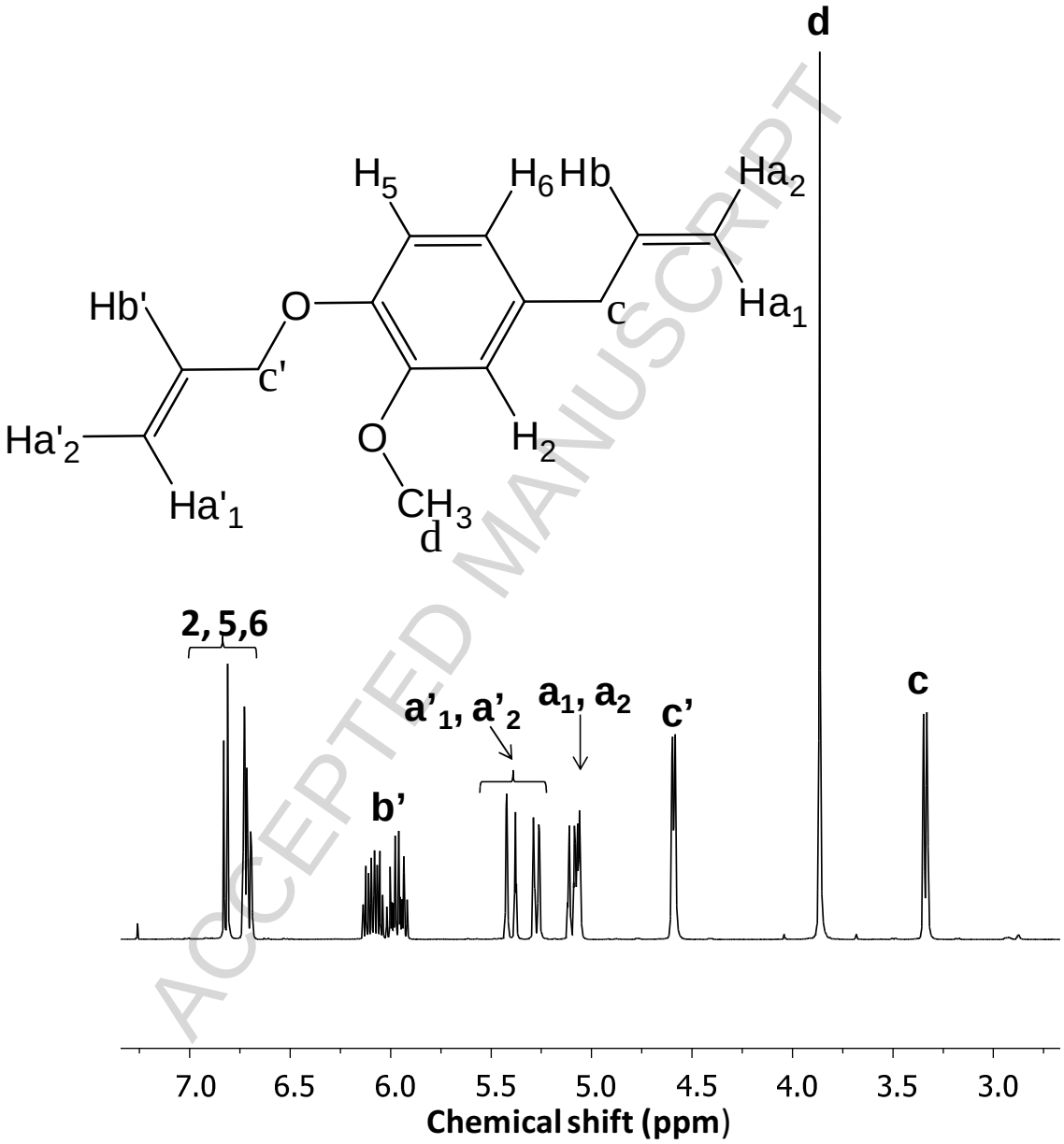

Figure 2. FTIR spectra of allyl-eugenol ***AE***, linalool ***L*** and allyl-eugenol/linalool ***AE/L (70/30)*** in presence of trithiol before irradiation.

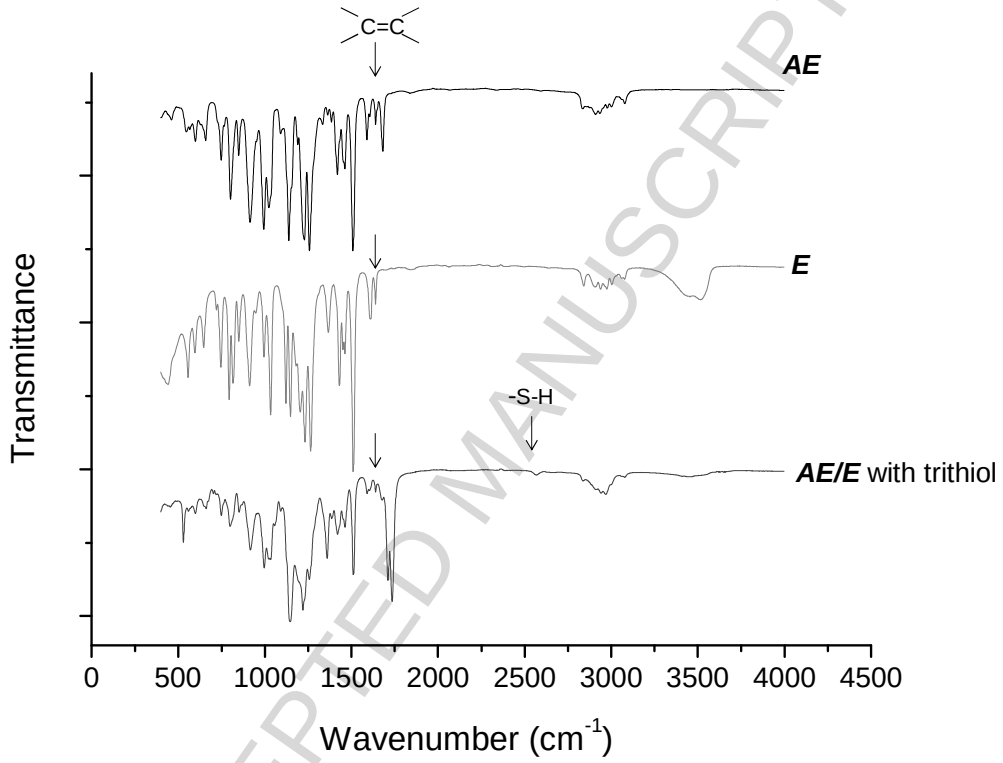

Figure 3. Real -time FTIR kinetic profiles of the formation of allyl-eugenol ***AE*** networks with trithiol in presence of DMPA in laminated conditions Xe-Hg lamp.

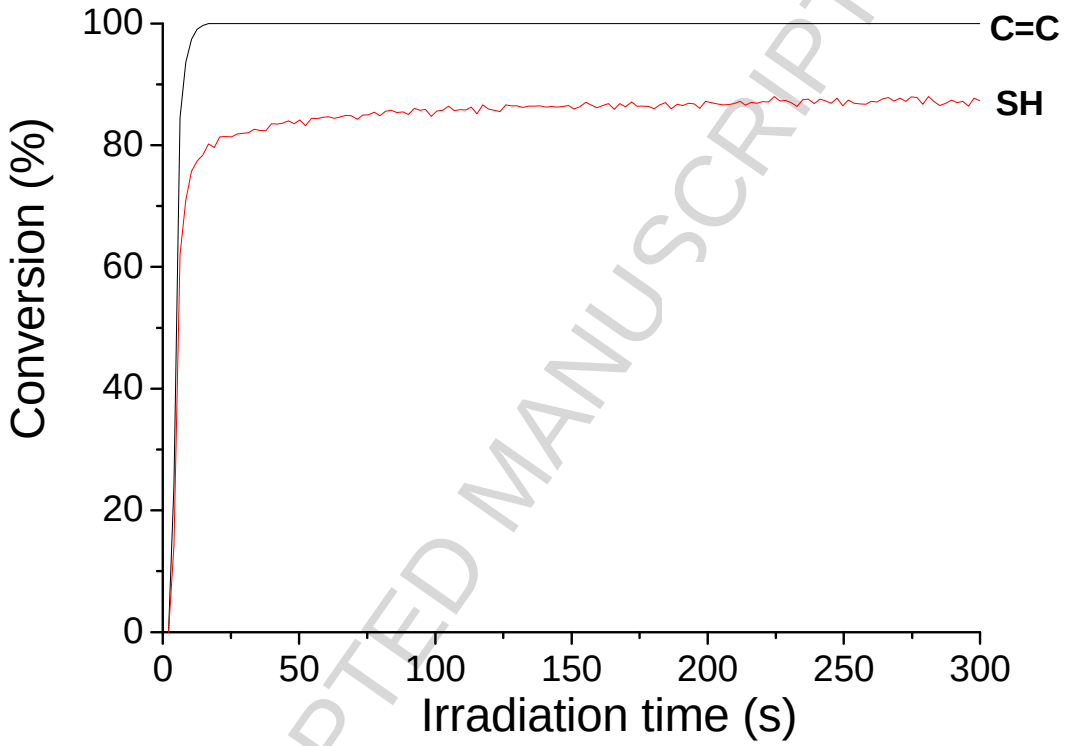

Figure 4. RAMAN spectra of ***AE/L (70/30***) (a) before and (b) after 300s of irradiation.

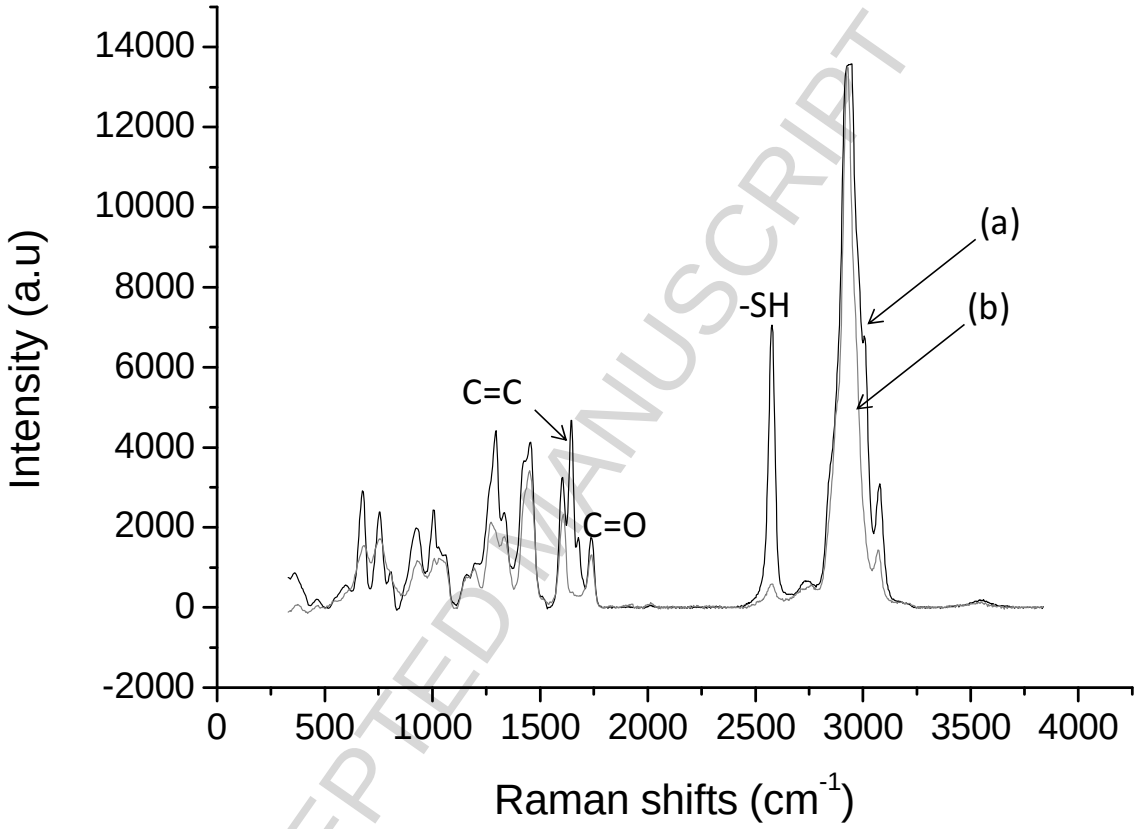

Figure 5. XPS spectra of (a) allyl-eugenol ***AE (100%)***, (b) allyl-eugenol/eugenol ***AE/E (70/30)***, (c) allyl-eugenol/linalool ***AE /L (70/30)*** and (d) allyl-eugenol/linalool ***AE /L (50/50)*** networks.

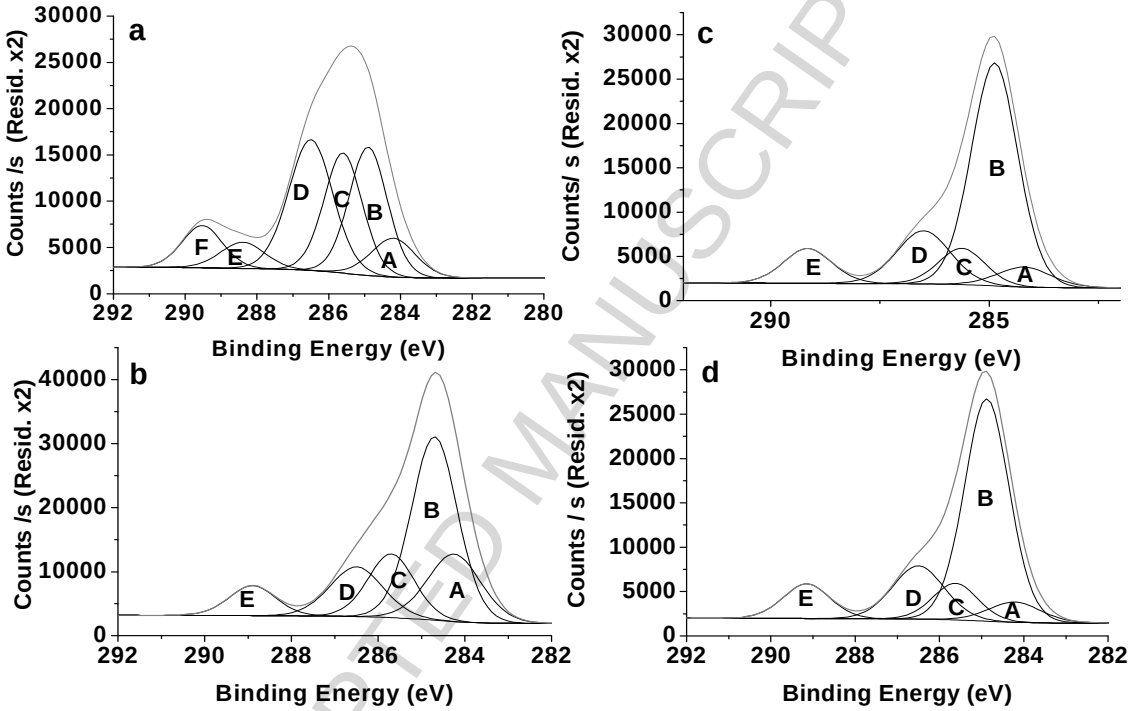

Figure 6. Tensile tests of (a) allyl-eugenol ***AE (100%)*** (b) allyl-eugenol/linalool ***AE/L (70/30)*** (c) allyl-eugenol/linalool ***AE/L (50/50)*** and (d) allyl-eugenol/eugenol ***AE/E (70/30)*** networks.

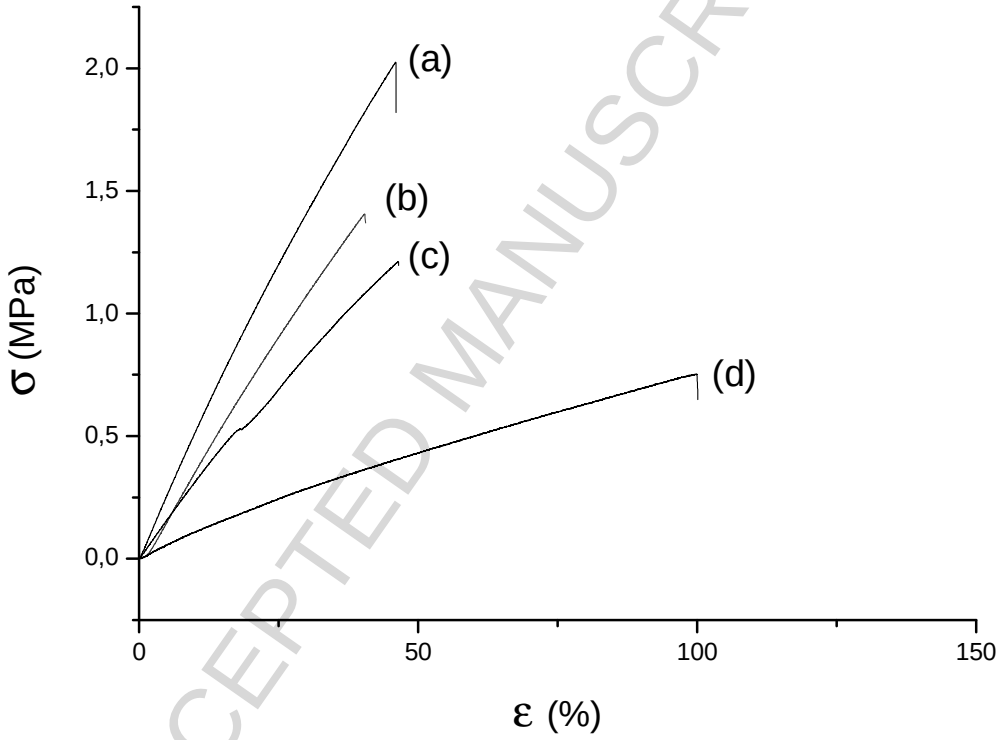

Figure 7. Antibacterial tests of allyl-eugenol/eugenol ***AE/E*** and allyl-eugenol/linalool ***AE/L*** networks.

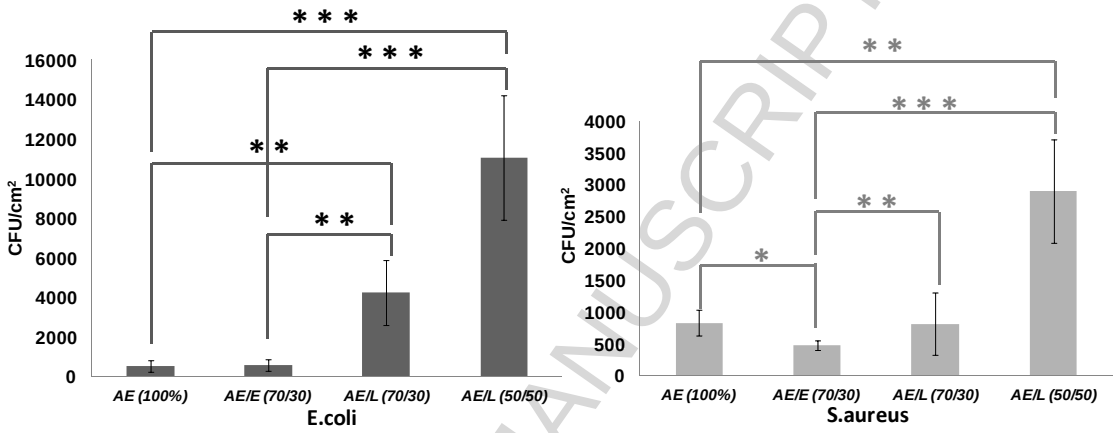

* Are statistically different with $p < 0.05$
* * Are statistically different with $p < 0.01$
* * * Are statistically different with $p < 0.001$

Figure 8. Antioxidant activity of the networks.

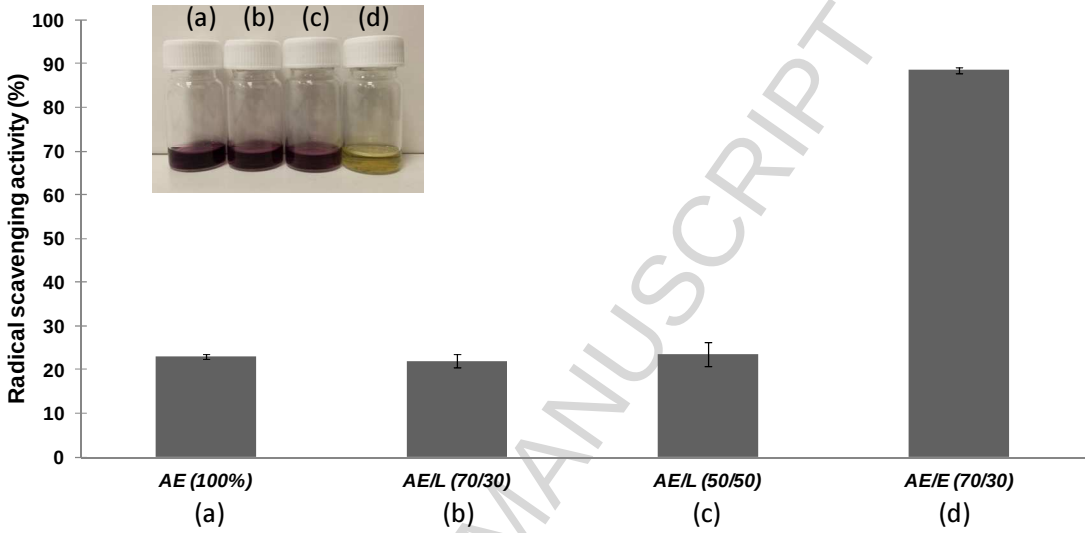

Table 1. Characteristics of allyl-eugenol/eugenol ***AE/E*** or allyl-eugenol/linalool ***AE/L*** networks .

Composition (w/w%)	***AE/L (100/0)***	***AE/L (70/30)***	***AE/E (70/30)***	***AE/L (50/50)***
Thickness (mm)	0.25 ± 0.01	0.43 ± 0.01	0.24 ± 0.03	0.34 ± 0.03
SH Conversion[a)] (%)	95	92	93	92
Soluble extract[b)] (%)	3	1	3	3

[a)] Determined by Raman
[b)] Determined by gravimetric analysis

Table 2. Characterization of ***AE-E*** or ***AE-L*** networks .

Composition (w/w%)	Tg[a)] (℃)	$T_{5\%}$[b)] (℃)	γ[c)] (°)	E[d)] (MPa)°	σ_R[d)] (MPa)	ε_R[d)] (%)	Water up take[e)] (%)
AE/E (100/0)	-1	323	73	5.1 ± 0.4	2.1 ± 0.1	48 ± 4	0.2
AE/L (70/30)	-5	301	70	3.7 ±0.3	2.7 ± 0.3	50 ± 6	0.4
AE/L (50/50)	-5	271	62	3.1 ± 0.2	2.3 ±0.1	50 ± 3	0.5
AE/E (70/30)	-4	305	83	1.1 ± 0.1	0.7 ± 0.02	92 ± 10	0.3

a) Determined by DSC
b) $T_{5\%}$: temperature of 5% weight loss of the networks determined by TGA
c) Determined by water contact measurements
d) Determined by tensile measurements
e) Determined by coulometry after 18h of exposure to water saturated air

Table 3. C1s peaks assignments and surface concentration of C1s peaks fitting (at. %)

Peak	A	B	C	D	E	F
Composition	C=C 284.2 eV	C-C/C-H 284.8 eV	C-O/C-OH aromatic 285.7 eV	C-O/C-OH aliphatic 286.4 eV	C=O 288.5 eV	π-π* 289.3 eV
AE/E (100/0)	8.6	24.7	23.1	29.1	5.8	8.6
AE/E (70/30)	17.1	46.5	16.2	12.6	7.6	
AE/L (70/30)	5.4	60.7	9.9	14.5	9.4	
AE/L (50/50)	6.2	58.5	9.6	16.2	9.4	